S6K1 Plays a Key Role in Glial Transformation

Jean L. Nakamura,[1] Edna Garcia,[1] and Russell O. Pieper[2]

Departments of [1]Radiation Oncology and [2]Neurological Surgery, University of California, San Francisco, California

Abstract

The mammalian target of rapamycin (mTOR) is a nutrient and ATP sensor suggested to play an important role in tumorigenesis, particularly in the setting of PTEN loss or activated Akt/PKB. Of mTOR's two known effectors, eIF4E has been implicated in tumorigenesis, whereas the role of S6 kinase (S6K1) in transformation is less understood. To assess the contribution of S6K1 to the transformed phenotype, we pharmacologically and genetically manipulated the mTOR-S6K pathway in glioma cells and monitored its effects on growth in soft agar, a hallmark of cellular transformation, and also assessed *in vivo* intracranial growth. Anchorage-independent growth by $HRas^{V12}$-transformed human astrocytes as well as by U251 and U373 human glioma cells was inhibited by pharmacologic mTOR inhibition. Similarly, short hairpin RNA–mediated suppression of mTOR also reduced anchorage-independent growth of glioma cell lines. Expression of wild-type eIF4E in rapamycin-treated E6/E7/hTert/$HRas^{V12}$ and U373 cells failed to rescue colony formation, although expression of wild-type S6K1 or rapamycin-resistant S6K1 in rapamycin-treated U373 and U251 provided partial rescue. Consistent with the latter observation, small interfering RNA–mediated suppression of S6K1 in $HRas^{V12}$-transformed human astrocytes, U251, and U373 cells resulted in a significant loss of anchorage-independent growth. Furthermore, we found that *in vivo* short hairpin RNA–mediated suppression of S6K1 in $HRas^{V12}$-transformed human astrocytes reduced intracranial tumor size, in association with reduced tumor levels of phosphorylated ribosomal protein S6. These findings implicate the mTOR-S6K pathway as a critical mediator of glial cell transformation. [Cancer Res 2008;68(16):6516–23]

Introduction

The mammalian target of rapamycin (mTOR) is an ATP and nutrient sensor that contributes to the control of cell size and cell cycle progression. mTOR's ability to control cell size and cell cycle is due at least in part to its ability to regulate the translation of specific classes of mRNAs. mTOR-mediated control of translation is a rapamycin-sensitive process accomplished by regulation of the downstream targets, S6K and eIF4E (1–3). mTOR phosphorylates S6K, leading to the phosphorylation of the ribosomal protein S6 and subsequent increased translation of mRNA with 5′ terminal oligopyrimidine sequences (2). In contrast, inhibition of eIF4E by the translational repressor 4EBP1 is reversed when 4EBP1 is phosphorylated by mTOR, resulting in the release of eIF4E, which can associate with eIF4A, eIF4G, and eIF4B to initiate the translation of capped mRNA (4).

The rapamycin-sensitive translational functions mediated by S6K and 4EBP1 have recently been recognized to be a result of mTOR's interaction with raptor to form the mTORC1 complex, whereas rapamycin-insensitive functions are a result of mTOR's interaction with rictor, forming mTORC2 (5–9). It remains to be determined how regulation of mTOR by raptor and rictor is coordinated, although each seems to control distinct and mutually exclusive mTOR functions. mTORC1, but not mTORC2, activates S6K, which can then inhibit insulin receptor substrate-I (IRS-1), thereby limiting insulin receptor–mediated signaling through phosphoinositide-3-kinase (PI3K). mTORC2, in contrast, has recently been shown to phosphorylate PKB at Ser^{473}, thereby functioning as a PDK-2 (7).

Substantial indirect evidence indicates that mTOR fulfills a central role in tumor development and maintenance. Oncogenic signaling through a variety of molecules, such as the epidermal growth factor receptor, Ras, and PI3K, can up-regulate mTOR activity and promote neoplastic growth (10). Tumors lacking normal Akt control mechanisms have also been shown to be particularly vulnerable to mTOR inhibition (11) and evidence of elevated mTOR activity can be found in multiple types of tumors (12), including malignant gliomas (13). These findings have led to the idea that mTOR plays a role in tumor maintenance, and to the development of mTOR inhibitors as systemic therapy against a wide range of malignancies.

Despite evidence of a link between mTOR, S6K, and eIF4E in response to growth factor activation, it is unclear whether S6K and/or eIF4E connect mTOR to tumor development and growth. Evidence from model systems has implicated eIF4E and S6K in tumor development in specific oncogenic contexts. For example, overexpression of eIF4E has been shown to transform rat fibroblasts in cooperation with v-myc or E1A, and *in vivo* eIF4E overexpression causes the development of lymphomas, angiosarcomas, lung adenocarcinomas, and hepatocellular adenomas (14–17). Inhibition of cap-binding by eIF4E also suppresses eIF4E-driven transformation (15). Although S6K has not been described as an oncoprotein, phosphorylated S6 protein levels are elevated in various tumor types, including malignant glioma (13, 18), and translational targets of S6K such as HIF1α seem to be critical in supporting tumor growth (19). Tumors with elevated HIF1 are sensitive to mTOR inhibition, and expression of HIF1α 5′-TOP sequences confers sensitivity to the mTOR inhibitor CCI-779 (20). Recent data also indicates that inhibition of angiogenesis by the tumor suppressor promyelocytic leukemia protein is in part dependent on its ability to inhibit mTOR and the synthesis of HIF1α (21). Although these data suggest that eIF4E and S6K may directly mediate transformation through mTOR, amplification or mutation of eIF4E or S6K has not been found in spontaneously arising tumors, nor is mTOR itself thought to be an oncogene. Thus, the contribution of eIF4E and S6K to mTOR-dependent glial transformation remains open.

Requests for reprints: Jean L. Nakamura, Department of Radiation Oncology, University of California, San Francisco, 505 Parnassus Avenue, Long Hospital L-75, San Francisco, CA 94143. Phone: 415-353-9694; Fax: 415-353-9883; E-mail: jnakamura@radonc.ucsf.edu.

doi:10.1158/0008-5472.CAN-07-6188

In order to test whether mTOR-dependent transformation requires both eIF4E and S6K functions, we genetically and pharmacologically manipulated mTOR and its downstream effectors and monitored its effects on the transformation status of human glioma cell lines and transformed human astrocytes. We found that suppression of mTOR or raptor was sufficient to significantly reduce anchorage-independent growth in soft agar, an assay of transformation. Furthermore, S6K1, but not eIF4E, rescued glioma growth in soft agar from rapamycin-mediated suppression, and transient S6K1 inhibition was sufficient to significantly reduce glioma growth in soft agar. *In vivo* S6K1 suppression in intracranially implanted glioma xenografts reduced levels of phosphorylated S6 and also resulted in reduced intracranial tumor growth. This data is the first direct demonstration of S6K's importance in supporting tumor growth both *in vitro* and *in vivo*. Collectively, these findings define a significant role for the mTOR-raptor (mTORC1)-S6K pathway in supporting gliomagenesis.

Materials and Methods

Cells and cell culture. Human glioma cell lines were obtained from the Brain Tumor Research Center Tissue Bank at the University of California, San Francisco. Immortalized human astrocytes and $HRas^{V12}$- and $HRas^{V12}$/Akt-transformed human astrocytes (E6/E7/hTert, E6/E7/hTert/$HRas^{V12}$ and E6/E7/hTert/$HRas^{V12}$/Akt, respectively) were generated as previously described (22, 23). All cell lines were grown in DMEM (4,500 mg/L glucose; Life Technologies, Inc.) supplemented with 10% fetal bovine serum (Life Technologies, Invitrogen), penicillin, and streptomycin. Cells were grown in a humidified incubator containing 8% carbon dioxide at 37°C.

Proliferation assay. To assess cell proliferation, the 3-(4-5-dimethylthiazol-2-yl)-5-(3-carboxymethoxyphenyl)-2-(4-sulfophenyl)-2H-tetrazolium salt (MTS) assay was used (CellTiter96; Promega). Cells were plated in triplicate into 96-well plates at a concentration of 2,000 cells/well (100 μL/well). At specified time points, 20 μL of MTS reagent were added to each well and allowed to incubate for 1 h. Absorbance (490 nm) was then determined in a 96-well plate reader.

Plasmids, transfection, and selection of cells. A pCAN1 vector encoding wt-eIF4E was a gift from Frank McCormick (University of California, San Francisco, San Francisco, CA). To generate a construct permitting wt-eIF4E expression with a unique selectable marker in E6/E7/hTert/$HRas^{V12}$ and E6/E7/hTert/$HRas^{V12}$/Akt cells, wt-eIF4E was subcloned from pCAN1-wt-eIF4E into the retroviral vector pMXI, which encodes green fluorescent protein (GFP) as a marker. Subcloning was performed as follows: pCAN1-wt-eIF4E was digested with *Xho*I and *Eco*RI, followed by gel purification of the wt-eIF4E encoding insert and ligation of the insert into identically digested pMXI. The retroviral pBABE constructs encoding wild-type S6K1 or rapamycin-resistant S6K (pBABE/F5A-E389) were gifts from John Blenis (Harvard Medical School, Boston, MA). Retroviral vectors were used to infect cells as previously described (22). Small interfering RNA (siRNA) targeting S6K1 (Ambion), 4EBP1 (Ambion), and control scramble sequence (Ambion) were transfected using FUGENE 6 (Roche). Monolayer cells, grown to ~80% confluence, were exposed to retroviral supernatants with 8 μg/mL of polybrene. Pools of productively infected cells (obtained by selection with puromycin or hygromycin) were used for further analyses. Cells expressing GFP were separated by fluorescence-activated cell sorting (FACS) on a FACSVantage sorter (Becton Dickinson) located in the UCSF Laboratory for Cell Analysis at a band-pass filter of 530/30 nm. Sorting gates were set such that 99% of the negative population and <1% of the positive population were excluded from the collection. Pooled collected cells were used for further analyses.

Lentiviral production and infection. Lentiviral short hairpin RNAs (shRNA) targeting mTOR (6) was obtained from Addgene, Inc. The lentivirus was packaged by cotransfection of 293T cells with the shRNA expression vector, vesicular stomatitis virus-glycoprotein, and Δ-VPR plasmids at a ratio of 1:0.9:0.1, using FUGENE 6 (Roche). Forty-eight hours after transfection, the supernatants containing lentiviral particles were harvested. Monolayer cells, grown to ~80% confluence, were exposed to the above lentiviral supernatants in the presence of 8 μg/mL of polybrene for 48 h, followed by selection with 2 μg/mL of puromycin for 1 week. After antibiotic selection, pools of productively infected cells were used for further analyses.

S6K1 was silenced in a tetracycline-inducible fashion by cloning a 97mer hairpin oligonucleotide targeting the S6K1 transcript into the pPRIME Tet-inducible construct (24). The following sequence was used to generate shRNA targeting S6K1: forward 5′-CCCCTGTCAGCCCAGTCAAATTTTCAAGAGAAATTTGACTGGGCTGACAG TTTTT-3′, reverse 3′-GGGGACAGTCGGGTCAGTTTAAAAGTTCTCTTTAAACTGACCCGACTTCAAAAA-5′. This sequence was cloned into pPRIME Tet-GFP-FF3 (a kind gift from Stephen J. Elledge, Harvard University) producing pPRIME Tet-GFP-S6K1 (SCT). The cloning product was confirmed by sequencing, virus was generated as described above, and 293T cells were infected with either pPRIME Tet-GFP-FF3 (targeting firefly luciferase, 8 μg of vesicular stomatitis virus-glycoprotein, 8 μg of pCMV, and 16 μg of lentiviral vector, and used as a negative control) or pPRIME Tet-GFP-SCT. Viral supernatant was concentrated using Centricon Plus-20 filters (Millipore), then added to $HRas^{V12}$-transformed human astrocytes. After 4 days of incubation, infected cells were sorted for GFP expression, and this GFP-positive pooled population was maintained in standard culture conditions described above. Doxycycline (Sigma-Aldrich) at 5 μg/mL in standard medium was added to induce the expression of shRNA in culture.

Soft agar colony formation assay. As previously described (22), cells (1×10^4) were plated in DMEM plus 10% FCS in 0.35% (w/v) low-melting temperature agar between layers of 0.7% low-melting temperature agar. After 3 weeks, colonies were stained with 3-(4,5-dimethylthiazol-2-yl)-2,5-diphenyltetrazolium bromide (Sigma-Aldrich) and colonies of >50 cells were scored by counting under a microscope. All experiments were performed at least in quadruplicate.

Animal injection. Immunodeficient rats (*rnu/rnu*; National Cancer Institute) were injected intracranially as described previously (22) with $HRas^{V12}$-transformed human astrocytes expressing either control lentivirus (Ras Tet) or SCT (Ras SCT). Three days after injection, animals were fed either LabDiet 5053 or LabDiet 5053 (Purina) supplemented with doxycycline at 6,000 ppm daily. After 14 days of exposure to doxycycline or control feed, animals were sacrificed, perfused with 4% paraformaldehyde, and brains were fixed in paraformaldehyde and paraffin-embedded.

Immunoblot analysis. Cells were harvested in lysis buffer [150 mmol/L NaCl, 20 mmol/L Tris-HCl (pH 7.5), 1% NP40, 1 mmol/L EDTA, 1 mmol/L EGTA, 1 mmol/L sodium orthovanadate, and protease inhibitor mixture (Boehringer Mannheim, Co.)] at 4°C. Lysate was centrifuged (12,000 × *g*) for 10 min at 4°C to remove insoluble components. Protein was quantitated by the Bio-Rad Dc protein assay. Equal amounts of protein were separated on SDS-PAGE 12% to 16% gels, then transferred to Immobilon-P polyvinylidene difluoride membrane (Millipore). The membrane was blocked with 5% nonfat dry milk in TBS containing 0.1% Tween 20. The membrane was then incubated with primary antibody in TBST, followed by secondary antibody linked to horseradish peroxidase diluted in TBST. ECL Detection System for Western blot Analysis (Amersham) was used according to the manufacturer's instructions for antibody detection. An AlphaImager 2000 Documentation and Analysis System (Multi Image light cabinet photodensitometer) was used to quantify the appropriate bands (Alpha Innotech Corporation). Primary antibodies used were anti-raptor, anti-mTOR, anti-S6K, anti–phosphorylated p70S6K Thr^{389}, anti-phosphorylated S6 $Ser^{235/236}$ (all from Cell Signaling), and anti–α-tubulin (Santa Cruz Biotechnology).

Immunohistochemistry. Five-micrometer sections were obtained through paraffin-embedded brain tumors at intervals of 500 μm. Sections were stained with H&E, and the maximum cross-sectional dimension of the tumor was measured under a microscope by an observer blinded to treatment. The maximal tumor area was calculated on each consecutive slide through the tumors and summed for each tumor. Phosphorylated S6 $Ser^{235/236}$ (Cell Signaling) was assessed on paraffin-embedded sections using

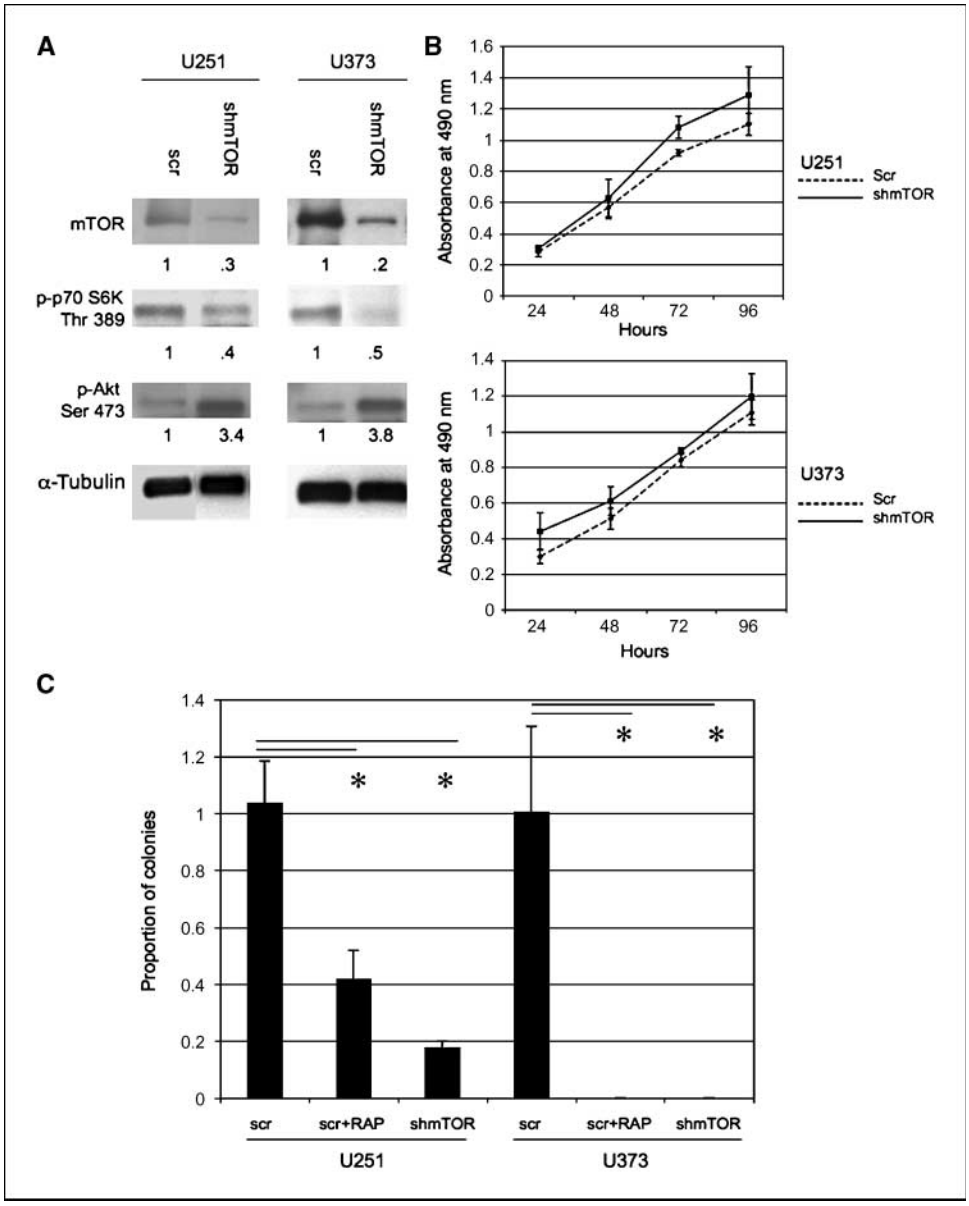

Figure 1. Reduction in mTOR protein levels suppresses soft agar colony formation. *A,* U251 and U373 cells were infected with lentivirus encoding either a scrambled shRNA (*scr*) or shRNA targeting mTOR (*shmTOR*). After antibiotic selection, whole cell lysate from each cell line was assessed by immunoblotting for levels of mTOR, phosphorylated p70S6K Thr^{389}, phosphorylated Akt Ser^{473}, and α-tubulin. Equal loading was verified by α-tubulin. *B,* cells expressing either shRNA targeting mTOR or raptor were plated at equal densities in 96-well plates, and proliferation was assessed over 96 h by the MTS assay. Proliferation slopes of each cell line are comparable, indicating that proliferation rates are not significantly altered by mTOR or raptor suppression. *C,* cells expressing either scrambled shRNA or shRNA targeting mTOR were plated in soft agar. Cells expressing scrambled shRNA were incubated with vehicle or 100 nmol/L of rapamycin, whereas cells expressing shRNA targeting mTOR were incubated without rapamycin. After 3 wk of incubation, cells were stained and the number of colonies was counted. *Columns,* mean number of colonies produced per cell line; *bars,* SE (*, $P < 0.05$, Student's *t* test).

immunofluorescent staining as described previously (25). Images were captured and merged using Openlab (Improvision).

Statistics. Statistical analyses were performed using the GB-STAT statistical package (Dynamic Microsystems). Standard errors were calculated for each mean, and statistical differences between groups were determined by Student's *t* test or ANOVA followed by Newman-Keul post hoc tests as indicated.

Results

Anchorage-independent growth of human glioma cells is dependent on mTOR-raptor signaling. Anchorage-dependent growth by tumors displaying activated PKB/Akt signaling, such as those lacking PTEN, is sensitive to mTOR inhibition (11), although mTOR's role in maintaining anchorage-independent growth is less well defined. We used the mTOR inhibitor rapamycin to assess whether the anchorage-independent growth of two human glioma cell lines and two transformed human astrocytic cell lines was mTOR-dependent. Immortalized human astrocytes transformed by the expression of HRas^{V12} or HRas^{V12}/Akt grew in soft agar as did the U251 and U373 glioblastoma cell lines. The addition of rapamycin in the agar, however, suppressed the colony-forming ability of all cells (data not shown). The anchorage-independent growth of HRas^{V12}/Akt-transformed human astrocytes was also no more resistant to rapamycin than that of human astrocytes transformed by HRas^{V12} alone, indicating that activated Akt failed to rescue anchorage-independent growth from suppression by rapamycin.

To confirm these results, we also determined whether specific suppression of mTOR altered the growth of glioma cell lines in soft agar. To do so, we stably introduced lentivirus encoding shRNA targeting mTOR in U251 and U373, then assessed levels of mTOR and the downstream effectors phosphorylated p70S6K Thr^{389} and phosphorylated Akt Ser^{473} by Western blotting. As shown in Fig. 1*A*, shRNA targeting mTOR selectively suppressed mTOR levels in both cell lines, leading to decreased phosphorylated p70S6K Thr^{389} levels. Consistent with prior observations, we also observed a

concomitant increase in phosphorylated Akt Ser^{473} (26). Although suppression of mTOR in cell lines did not significantly alter the proliferation rates of cells in culture (Fig. 1*B*), it did suppress the growth of cells in soft agar (relative to scramble control) to an extent comparable to the loss of growth observed with rapamycin exposure (Fig. 1*C*). These results show that mTOR plays a key role in maintaining anchorage-independent growth and transformation in glioma cells.

eIF4E expression fails to reverse rapamycin-mediated suppression of anchorage-independent growth. Because eIF4E has been shown to play a role in the transformation of 3T3 cells and in leukemogenesis, we expressed wild-type eIF4E in HRas^{V12}-transformed human astrocytes, HRas^{V12}/Akt-transformed human astrocytes, and U373 cells, then assessed the ability of eIF4E to alter the effects of rapamycin on growth in soft agar. As shown in Fig. 2*A*, retroviral infection of HRas^{V12}, HRas^{V12}/Akt-transformed human astrocytes, and U373 cells increased eIF4E expression relative to vector control cells. eIF4E expression in HRas^{V12}/Akt-transformed human astrocytes significantly increased colony formation in the absence of rapamycin relative to vector control cells (Fig. 2*B*). eIF4E expression did not, however, reverse rapamycin-mediated suppression of colony formation in soft agar (Fig. 2*B*). In contrast to the effects of eIF4E expression in HRas^{V12}-transformed human astrocytes, eIF4E expression in U373 did not alter baseline soft agar colony formation. However, as in the above cell lines, eIF4E expression in U373 failed to confer resistance to rapamycin exposure. These data indicate that whereas eIF4E introduction confers a growth advantage, it does not rescue cells from rapamycin-induced suppression of growth in soft agar.

eIF4E function is negatively regulated by 4EBP1, and we further substantiated the above finding by silencing 4EBP1 in HRas^{V12}-transformed human astrocytes and U251 using siRNA (Fig. 2*C*), then assessing the ability of 4EBP1 to alter the effects of rapamycin on growth in soft agar. Reduction of 4EBP1 levels in both cell lines failed to rescue cells from the effects of rapamycin in soft agar (Fig. 2*D*), providing further support that eIF4E does not significantly support mTOR-driven growth by gliomas.

S6K supports anchorage-independent growth. S6K has been shown to modulate the translation of messages possessing 5′-TOP sequences, but has not been implicated in tumorigenesis. To directly address the role of S6K in transformation, we expressed wild-type S6K, or a constitutively active, rapamycin-resistant mutant S6K (E389R) in U373 and U251, then assessed its effects on growth in soft agar with and without rapamycin present. As

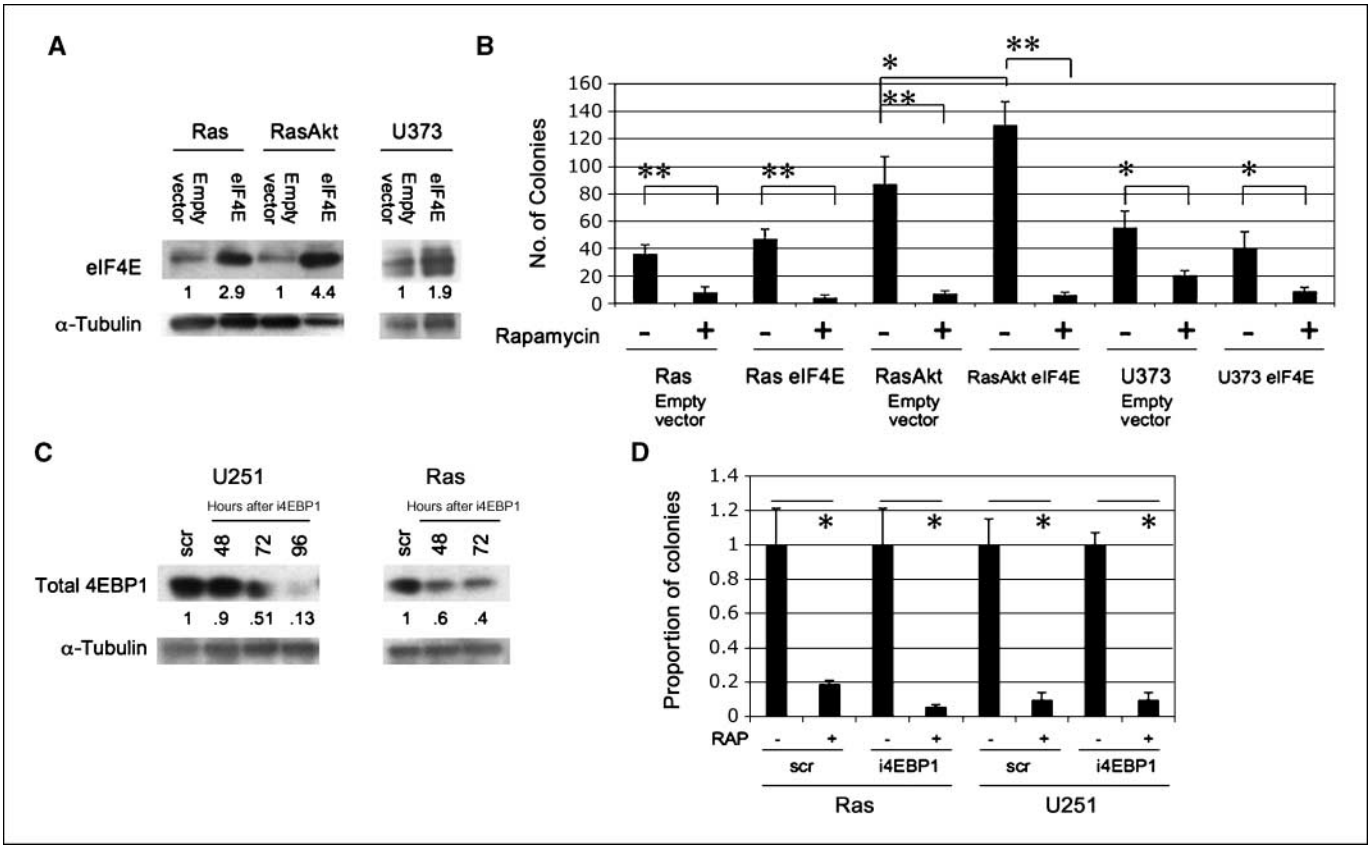

Figure 2. Neither eIF4E expression nor 4EPBP1 suppression are sufficient to rescue anchorage-independent growth from rapamycin. *A,* human astrocytes transformed by HRas^{V12}, or HRas^{V12}/Akt, and human glioma U373 cells were infected with either an empty vector encoding GFP or vector encoding GFP and wild-type eIF4E. After cells were FACS-sorted to isolate GFP-positive cells, whole cell lysate from the cell lines were assessed by immunoblotting for total eIF4E protein. Equal loading was verified by α-tubulin. *B,* cells expressing either wild-type eIF4E or empty vector were plated in soft agar in the presence or absence of 100 nmol/L of rapamycin, then after 3 wk of incubation, cells were stained and colonies were counted. *Columns,* mean number of colonies produced per cell line; bars, SE (*, $P < 0.05$ and **, $P < 0.01$, two-way ANOVA followed by Neuman-Keuls post hoc test). *C,* U251- and HRas^{V12}-transformed human astrocytes were transfected with either scramble control (*scr*) or siRNA against 4EBP1 (*i4EBP1*). Whole cell lysates collected at specified time points were assessed by immunoblotting for total 4EBP1 and α-tubulin. *D,* cells transfected with either i4EBP1 or scramble control were plated in soft agar 24 h after transfection (in the absence or presence of rapamycin) and scored for colony numbers after 3 wk of incubation. *Columns,* mean proportion of colonies produced per cell line, normalized to untreated controls; *bars,* SE (*, $P < 0.05$; Student's *t* test).

shown in Fig. 3*A*, introduction of a vector encoding wild-type or constitutively activated S6K (E389R) increased levels of S6K and phosphorylated S6 $Ser^{235/236}$ 2-fold to 3-fold in both cell lines relative to empty vector cells (pBabe). Having confirmed protein expression in viral transfectants, pooled transfectants were grown in soft agar in the presence or absence of rapamycin, and colonies were counted after 3 weeks. As shown in Fig. 3*B*, colony formation by U251 cells expressing wild-type S6K remained sensitive to rapamycin exposure, whereas colony formation by U251 cells expressing the mutant S6K E389R was resistant to the presence of rapamycin. In U373 cells, expression of either wild-type S6K or the mutant S6K E389R resulted in partial rescue of soft agar colony formation in the presence of rapamycin, as compared with the empty vector (Fig. 3*B*). The reduced expression of wild-type S6K, compared with the expression of mutant S6K E389R in the U251 cells, may explain the absence of rescue from rapamycin-mediated suppression of soft agar growth that was observed in the U251 as compared with the U373 cells which, in comparison, had more comparable protein levels of the wild-type and mutant forms of S6K. To further assess S6K's importance in maintaining a transformed state, we performed the converse experiment by transiently transfecting U373, U251, and $HRas^{V12}$-transformed human astrocytes with siRNA targeting S6K1, plating cells 24 hours after transfection into soft agar and monitoring colony formation 3 weeks later. As shown in Fig. 4*A*, siRNA transfection produced an ~50% to 70% reduction of total S6K1 protein levels in all three cell lines by 96 hours after transfection, and a 50% to 70% reduction in phosphorylated S6 $Ser^{235/236}$ levels. Cells transfected with siRNA targeting S6K1 grew to confluence at a similar rate as cells transfected with scramble control (data not shown). Consistent with the idea that S6K1 maintains anchorage-independent growth, however, S6K1 suppression was associated with a significant loss of colony formation in soft agar by U373, U251, and $HRas^{V12}$-transformed human astrocytes (Fig. 4*B*).

Because transient S6K1 knockdown significantly reduced anchorage-independent growth in all three cell lines tested, we sought to determine whether S6K1 knockdown *in vivo* could similarly inhibit tumor growth. However, concerns regarding the appropriateness of transient RNAi, as performed above, for *in vivo* studies of orthotopic xenografts led us to favor a more stable and inducible system for RNAi-based experiments. To confirm our *in vitro* findings, we constructed a lentiviral construct encoding shRNA targeting S6K1 in a tetracycline-inducible fashion and expressed either this construct or control vector into $HRas^{V12}$-transformed human astrocytes. Pooled cells expressing the constructs were isolated by FACS for GFP expression, and tetracycline-inducible iS6K1 was confirmed *in vitro* (Fig. 5*A*). $HRas^{V12}$-transformed human astrocytes expressing either control vector (Ras Tet) or vector targeting S6K1 (Ras SCT) were injected intracranially into rats. Based on previously described formulations for doxycycline-impregnated rodent feed (27), mice were exposed to either control feed or feed containing doxycycline. After a 14-day exposure to either control feed or feed containing doxycycline, animals were sacrificed and brains were fixed, sectioned and stained with H&E. We then assessed *in vivo* phosphorylated S6 $Ser^{235/236}$ levels by immunohistochemistry, and found that Ras SCT and Ras Tet tumors showed comparable levels of cytoplasmic phosphorylated S6 in the presence of control feed (Fig. 5*B*). Although exposure to doxycycline failed to alter levels of cytoplasmic phosphorylated S6 in Ras Tet tumors, Ras SCT tumors exposed to doxycycline had comparatively reduced cytoplasmic phosphorylated S6 (Fig. 5*A*). Animals injected with Ras SCT tumors and receiving doxycycline feed developed smaller tumors as compared with control animals (Fig. 5*C*, $P < 0.05$, Student's t test). Similar to the degree of reduced soft agar colony formation after iS6K shown in Fig. 4*B*, we observed ~50% smaller tumors in the animals injected with Ras SCT tumor cells and receiving doxycycline feed relative to controls. These data indicate that $HRas^{V12}$-transformed human astrocytes showed significant cytoplasmic levels of phosphorylated S6 *in vivo*, and suggest that S6K1 knockdown occurred in a doxycycline-dependent manner. These results show that maintenance of S6K1 activity supports $HRas^{V12}$ transformation *in vivo*, and that loss of S6K1 activity compromises tumor growth.

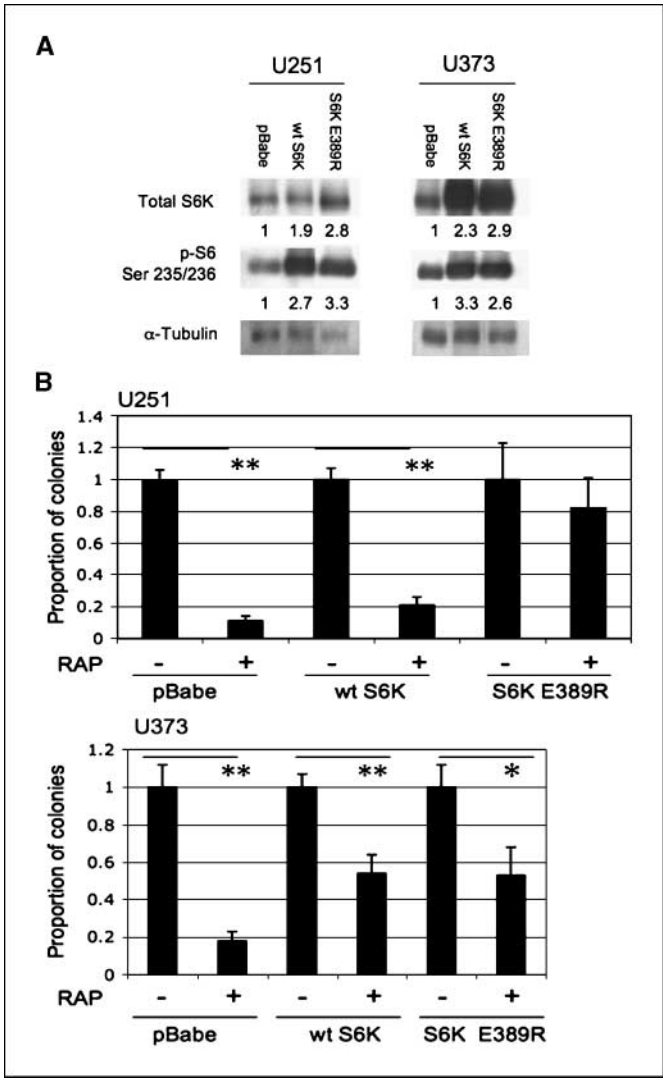

Figure 3. S6K1 supports mTOR-dependent anchorage-independent growth. *A,* U251 and U373 were transfected with either empty vector (*pBabe*), or vector encoding wild-type S6K1 (*wt S6K*), or constitutively active S6K1 (*S6K E389R*). After selection, whole cell lysates from each cell line were assessed by immunoblotting for total S6K, phosphorylated S6 $Ser^{235/236}$, and α-tubulin. Equal loading was verified by α-tubulin. *B,* U251 and U373 expressing wild-type S6K, constitutively active S6K E389R, or empty vector (pBabe) were plated in soft agar in the presence of rapamycin, and after 3 wk of incubation, cells were stained and colonies were counted. *Columns,* mean number of colonies produced per cell line; *bars,* SE (*, $P < 0.05$ and **, $P < 0.01$, two-way ANOVA followed by Neuman-Keuls post hoc test).

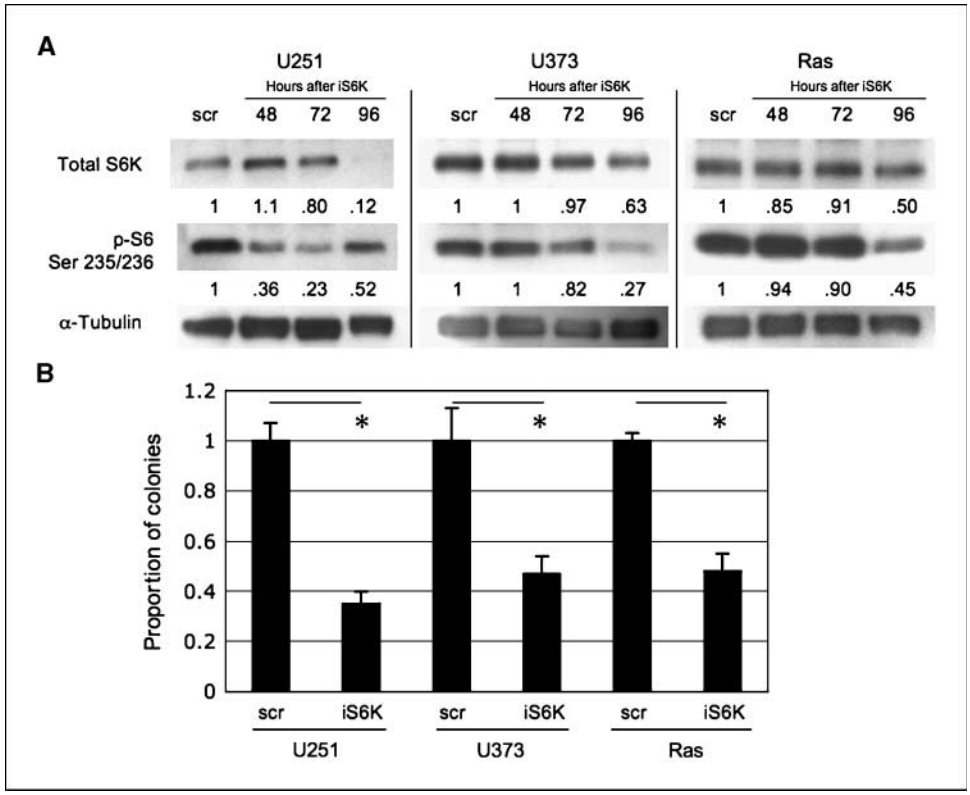

Figure 4. Reduction of S6K1 reduces tumor growth *in vitro* and *in vivo. A,* U251, U373, and $HRas^{V12}$-transformed human astrocytes were transfected with either scramble control (*scr*) or siRNA against S6K (*iS6K*). Whole cell lysates collected at specified time points were assessed by immunoblotting for total S6K, phosphorylated S6 $Ser^{235/236}$ and α-tubulin. *B,* cells transfected with either iS6K or scramble control were plated in soft agar 24 h after transfection (in the absence of rapamycin) and scored for colony numbers after 3 wk of incubation. *Columns,* mean proportion of colonies produced per cell line, normalized to untreated control; *bars,* SE (*, $P < 0.05$; Student's *t* test).

Discussion

mTOR and its downstream effectors, eIF4E and S6K, have been implicated in cellular transformation, although their contribution to glial transformation remains undefined. In this work, we show that growth of glioma cells in soft agar, a stringent assay for transformation, is blocked by down-regulation of mTORC1 and that signaling through S6K, but not eIF4E, maintains glial transformation. We also show that *in vivo* suppression of S6K results in reduced intracranial glioma growth. These findings indicate that the S6K arm may have special significance in glial transformation.

Our data suggest that mTORC2 function is less significant in mTOR-dependent anchorage-independent growth for a few reasons. Rapamycin has been reported to have alternate effects on Akt phosphorylation; prolonged rapamycin exposure has been shown to inhibit the assembly of mTORC2, thereby inhibiting Akt (28), and mTOR inhibition has also been described to induce IRS-1, leading to Akt activation (26). In the human glioma cell lines U251 and U373, we found that suppression of mTOR resulted in a significant increase in phosphorylated Akt Ser^{473} as compared with cells expressing scramble control. Despite the increase in phosphorylated Akt Ser^{473}, mTOR knockdown nonetheless significantly compromised these cells' anchorage-independent growth. These data suggest that in gliomas, mTORC2 is not the dominant arm supporting mTOR-dependent transformation, although it is possible that mTORC2 has effects on tumorigenesis that are Akt-independent.

Our data also suggest that S6K and eIF4E have distinct roles in gliomagenesis. Although prior findings have shown that eIF4E transforms rat fibroblasts, we found that eIF4E expression in U373 glioma cells and $HRas^{V12}$- and $HRas^{V12}$/Akt-transformed human astrocytes failed to restore anchorage-independent growth in the setting of mTOR inhibition. Silencing 4EBP1 also failed to rescue anchorage-independent growth from rapamycin-mediated suppression. eIF4E overexpression, however, increased colony formation in $HRas^{V12}$/Akt-transformed human astrocytes, suggesting that eIF4E plays a positive role in transformation, and it is possible that eIF4E's effects on transformation require other mTOR-dependent pathways such as S6K1. Another reason we cannot fully exclude a role by eIF4E in glial transformation is that superphysiologic levels of eIF4E beyond the 2-fold to 4-fold increases generated in this study may be required for transformation. Malignant gliomas have been described immunohistochemically to express more eIF4E as compared with normal neuroglial cells (29), although the degree of eIF4E overexpression in malignant gliomas remains undefined.

Although S6K has not been shown to be an oncoprotein, in the human gliomas assessed in this study, S6K seemed to be a key factor in maintaining anchorage-independent growth. The actions of S6K shown in human astrocytes may indicate that S6K has differing roles in various tissue types: for example, S6K1 deletion blocks growth factor–stimulated hypertrophy in muscle but not in neurons (30). S6K has numerous downstream targets, among them mRNAs with 5′-TOP sequences, the protein products of which are starting to be understood. The critical targets of S6K are not well defined, although the present data clearly suggest that these targets may be distinct from those influenced by eIF4E, and may represent better therapeutic targets. It should be noted that whereas the mTOR-S6K pathway seems to be critical for the growth of cells in soft agar, transformation of glial cells requires a series of events (p53 inactivation, retinoblastoma inactivation, telomerase reactivation, Ras activation) to which the mTOR-S6K pathway is merely a contributor (22, 31). This observation is consistent with the finding that supplying S6K to rapamycin-treated cells only partially rescues growth. The present findings suggest that S6K, but not eIF4E, plays a key, although not sufficient, role in glial transformation.

In addition to our data, which shows an important role for S6K1 in supporting gliomagenesis *in vitro* and *in vivo*, recently published data describe ribosomal S6 kinase 2 (RSK2) as supporting anchorage-independent growth induced by tumor-promoting agents such as epidermal growth factor and 12-*O*-tetradecanoylphorbol-13-acetate (32). RSK2, a homologue of S6K1, is similarly activated by mitogens and is inhibited by rapamycin (33). Although both RSK2 and S6K1 phosphorylate S6 *in vivo*, these kinases do not seem to be functionally redundant for a few reasons. S6K1 knockout mice have a small-body phenotype, despite the finding that mouse embryo fibroblasts from these animals show normal S6 phosphorylation *in vivo*, suggesting that RSK2 does not completely duplicate S6K1's functions (34). Comparisons of amino acid sequences and localization between the two S6 kinases also suggest distinct functional differences (33, 35). It remains possible that S6K1 and RSK2 support tumor growth through similar mechanisms, and further studies defining the transformation-promoting effects common or specific to these kinases are needed.

Defining the role of the mTOR-S6K pathway in glial transformation may have an effect on the design and implementation of glioma therapies. Current targeted therapies are based on our knowledge of pathways thought to be critical for tumorigenesis and proliferation. This rationale has led to the clinical testing of signaling inhibitors such as Tarceva and CCI-779. Despite this mechanistic approach to drug development, these agents have shown only modest effects, and combinatorial strategies that inhibit multiple kinases (for example PI3K or Akt in combination with mTOR) show more promise than strategies employing single kinase inhibition (36, 37). In the case of Akt/mTOR combinatorial therapy, the fact that mTOR inhibition can induce Akt activation through IRS-1 may explain why targeting the same pathway at multiple sites is associated with better efficacy. Concerns have been raised that Akt activation with mTORC1

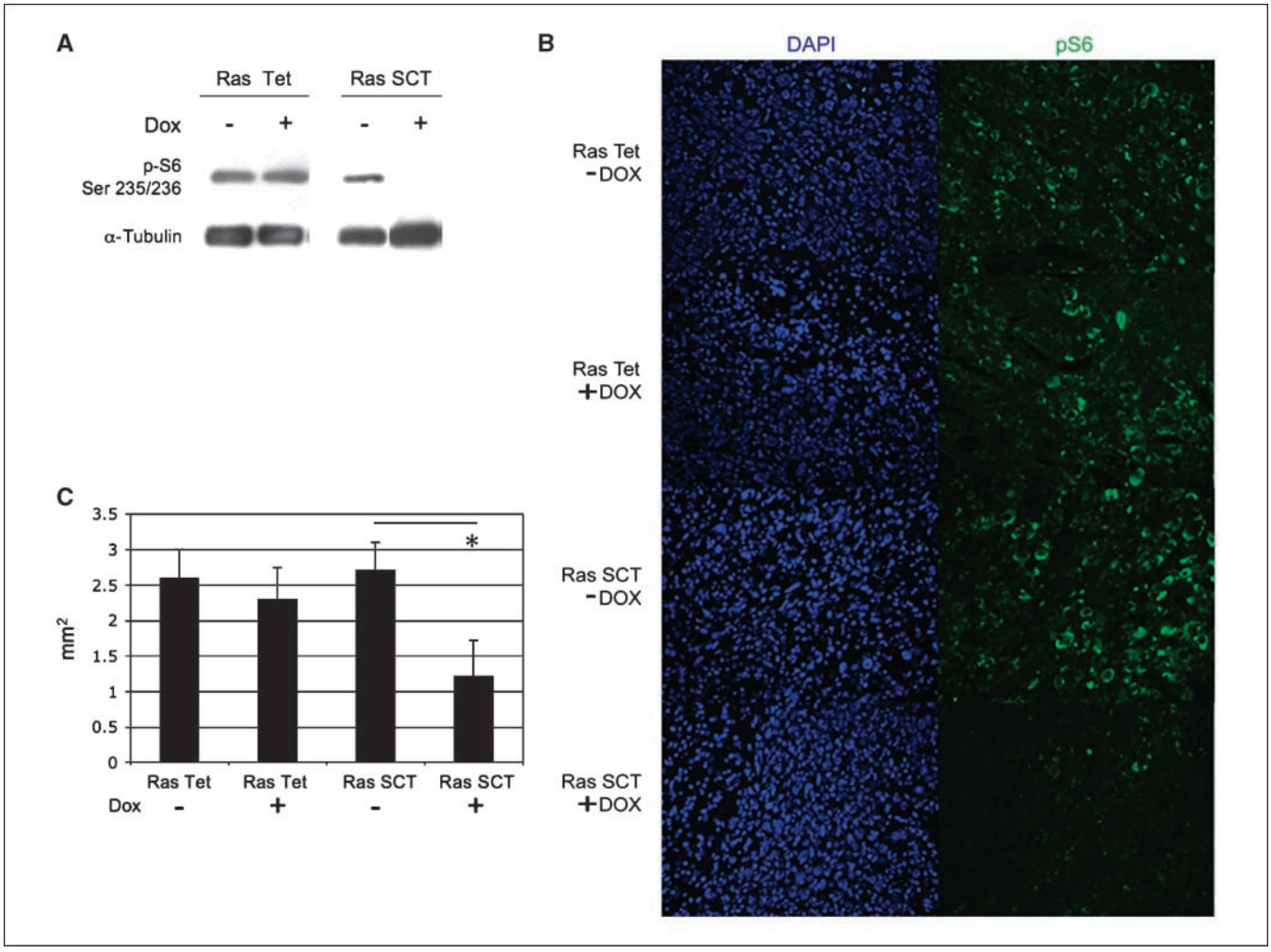

Figure 5. Reduction of S6K1 reduces tumor growth *in vivo*. *A,* short hairpin sequence targeting firefly luciferase (*control*) or S6K1 in a tetracycline-inducible lentiviral construct was expressed in $HRas^{V12}$-transformed human astrocytes (*Ras*). Cells were exposed to medium containing vehicle alone or doxycycline (5 μg/mL) for 4 d. Whole cell lysate from treated cells were assessed by immunoblotting for levels of phosphorylated S6 $Ser^{235/236}$. Equal loading was verified by α-tubulin. *B,* $HRas^{V12}$-transformed human astrocytes expressing either control vector (*Ras Tet*) or vector targeting S6K1 (*Ras SCT*) were injected intracranially in rats. After a 14-d exposure to either control feed or feed containing doxycycline (*−DOX* or *+DOX*), animals were sacrificed and brains were fixed and sectioned. Representative 5-μm sections through tumors were immunolabeled for phosphorylated S6 $Ser^{235/236}$ and stained with 4′,6-diamidino-2-phenylindole (*DAPI*). Fluorescence microscopy was used to visualize 4′,6-diamidino-2-phenylindole (*blue*) and phosphorylated S6 $Ser^{235/236}$ (*green*). Images were taken at ×20 magnification, and individual channels are displayed. *C,* 5-μm-thick coronal sections were taken at 0.5-mm intervals through the entire tumor, then stained with H&E. *Columns,* sum of maximum cross-sectional areas of tumors measured on consecutive coronal sections for each tumor; *bars,* SE (*, $P < 0.05$, Student's *t* test). Ras Tet ($n = 6$), Ras Tet +Dox ($n = 7$), Ras SCT ($n = 5$), and Ras SCT +Dox ($n = 6$).

inhibition could represent a mechanism for drug resistance and sustained tumor growth, although in our model, Akt activation did not rescue tumor growth from mTORC1 inhibition. Our observation that the mTOR-S6K pathway plays a key role in glial transformation suggests that targeting the Akt-mTOR-S6K pathway at a more distal point may be as effective as dual inhibition at a more proximal point. Selective S6K inhibitors are, at present, not available at the clinical or preclinical level, although the present study suggest that such agents, alone or in combination with other agents, might be rational choices for glioma therapy, and perhaps other tumors dependent on mTOR-S6K signaling for maintenance of the transformed phenotype.

Disclosure of Potential Conflicts of Interest

No potential conflicts of interest were disclosed.

Acknowledgments

Received 11/12/2007; revised 4/24/2008; accepted 5/25/2008.

Grant support: American Brain Tumor Association fellowship (J.L. Nakamura), American Cancer Society Institutional grant (J.L. Nakamura), 1K08CA115476-01 (J.L. Nakamura), and NIH Award R01CA94989 (R.O. Pieper).

The costs of publication of this article were defrayed in part by the payment of page charges. This article must therefore be hereby marked *advertisement* in accordance with 18 U.S.C. Section 1734 solely to indicate this fact.

References

1. Dennis PB, Jaeschke A, Saitoh M, Fowler B, Kozma SC, Thomas G. Mammalian TOR: a homeostatic ATP sensor. Science 2001;294:1102–5.
2. Fingar DC, Richardson CJ, Tee AR, Cheatham L, Tsou C, Blenis J. mTOR controls cell cycle progression through its cell growth effectors S6K1 and 4E-BP1/eukaryotic translation initiation factor 4E. Mol Cell Biol 2004;24:200–16.
3. Fingar DC, Salama S, Tsou C, Harlow E, Blenis J. Mammalian cell size is controlled by mTOR and its downstream targets S6K1 and 4EBP1/eIF4E. Genes Dev 2002;16:1472–87.
4. Gingras AC, Raught B, Sonenberg N. Regulation of translation initiation by FRAP/mTOR. Genes Dev 2001; 15:807–26.
5. Burnett PE, Barrow RK, Cohen NA, Snyder SH, Sabatini DM. RAFT1 phosphorylation of the translational regulators p70 S6 kinase and 4E-BP1. Proc Natl Acad Sci U S A 1998;95:1432–7.
6. Sarbassov DD, Ali SM, Kim DH, et al. Rictor, a novel binding partner of mTOR, defines a rapamycin-insensitive and raptor-independent pathway that regulates the cytoskeleton. Curr Biol 2004;14:1296–302.
7. Sarbassov DD, Guertin DA, Ali SM, Sabatini DM. Phosphorylation and regulation of Akt/PKB by the rictor-mTOR complex. Science 2005;307:1098–101.
8. Kim DH, Sabatini DM. Raptor and mTOR: subunits of a nutrient-sensitive complex. Curr Top Microbiol Immunol 2004;279:259–70.
9. Kim DH, Sarbassov DD, Ali SM, et al. mTOR interacts with raptor to form a nutrient-sensitive complex that signals to the cell growth machinery. Cell 2002;110: 163–75.
10. Aoki M, Blazek E, Vogt PK. A role of the kinase mTOR in cellular transformation induced by the oncoproteins P3k and Akt. Proc Natl Acad Sci U S A 2001;98:136–41.
11. Podsypanina K, Lee RT, Politis C, et al. An inhibitor of mTOR reduces neoplasia and normalizes p70/S6 kinase activity in Pten+/− mice. Proc Natl Acad Sci U S A 2001; 98:10320–5.
12. Vega F, Medeiros LJ, Leventaki V, et al. Activation of mammalian target of rapamycin signaling pathway contributes to tumor cell survival in anaplastic lymphoma kinase-positive anaplastic large cell lymphoma. Cancer Res 2006;66:6589–97.
13. Riemenschneider MJ, Betensky RA, Pasedag SM, Louis DN. AKT activation in human glioblastomas enhances proliferation via TSC2 and S6 kinase signaling. Cancer Res 2006;66:5618–23.
14. Cohen N, Sharma M, Kentsis A, Perez JM, Strudwick S, Borden KL. PML RING suppresses oncogenic transformation by reducing the affinity of eIF4E for mRNA. EMBO J 2001;20:4547–59.
15. Kentsis A, Topisirovic I, Culjkovic B, Shao L, Borden KL. Ribavirin suppresses eIF4E-mediated oncogenic transformation by physical mimicry of the 7-methyl guanosine mRNA cap. Proc Natl Acad Sci U S A 2004; 101:18105–10.
16. Ruggero D, Montanaro L, Ma L, et al. The translation factor eIF-4E promotes tumor formation and cooperates with c-Myc in lymphomagenesis. Nat Med 2004;10:484–6.
17. Lazaris-Karatzas A, Sonenberg N. The mRNA 5′ cap-binding protein, eIF-4E, cooperates with v-myc or E1A in the transformation of primary rodent fibroblasts. Mol Cell Biol 1992;12:1234–8.
18. Conde E, Angulo B, Tang M, et al. Molecular context of the EGFR mutations: evidence for the activation of mTOR/S6K signaling. Clin Cancer Res 2006;12:710–7.
19. Majumder PK, Febbo PG, Bikoff R, et al. mTOR inhibition reverses Akt-dependent prostate intraepithelial neoplasia through regulation of apoptotic and HIF-1-dependent pathways. Nat Med 2004;10:594–601.
20. Thomas GV, Tran C, Mellinghoff IK, et al. Hypoxia-inducible factor determines sensitivity to inhibitors of mTOR in kidney cancer. Nat Med 2006;12:122–7.
21. Bernardi R, Guernah I, Jin D, et al. PML inhibits HIF-1α translation and neoangiogenesis through repression of mTOR. Nature 2006;442:779–85.
22. Sonoda Y, Ozawa T, Hirose Y, et al. Formation of intracranial tumors by genetically modified human astrocytes defines four pathways critical in the development of human anaplastic astrocytoma. Cancer Res 2001;61:4956–60.
23. Sonoda Y, Ozawa T, Aldape KD, Deen DF, Berger MS, Pieper RO. Akt pathway activation converts anaplastic astrocytoma to glioblastoma multiforme in a human astrocyte model of glioma. Cancer Res 2001;61:6674–8.
24. Stegmeier F, Hu G, Rickles RJ, Hannon GJ, Elledge SJ. A lentiviral microRNA-based system for single-copy polymerase II-regulated RNA interference in mammalian cells. Proc Natl Acad Sci U S A 2005;102:13212–7.
25. Affara NI, Trempus CS, Schanbacher BL, et al. Activation of Akt and mTOR in CD34+/K15+ keratinocyte stem cells and skin tumors during multi-stage mouse skin carcinogenesis. Anticancer Res 2006;26: 2805–20.
26. O'Reilly KE, Rojo F, She QB, et al. mTOR inhibition induces upstream receptor tyrosine kinase signaling and activates Akt. Cancer Res 2006;66:1500–8.
27. Wang S, Khan A, Lang FF, Schaefer TS. Conditional gene expression in human intracranial xenograft tumors. Biotechniques 2001;31:196–202.
28. Sarbassov DD, Ali SM, Sengupta S, et al. Prolonged rapamycin treatment inhibits mTORC2 assembly and Akt/PKB. Mol Cell 2006;22:159–68.
29. Gu X, Jones L, Lowery-Norberg M, Fowler M. Expression of eukaryotic initiation factor 4E in astrocytic tumors. Appl Immunohistochem Mol Morphol 2005;13:178–83.
30. Chalhoub N, Kozma SC, Baker SJ. S6k1 is not required for Pten-deficient neuronal hypertrophy. Brain Res 2006;1100:32–41.
31. Rich JN, Guo C, McLendon RE, Bigner DD, Wang XF, Counter CM. A genetically tractable model of human glioma formation. Cancer Res 2001;61:3556–60.
32. Cho YY, Yao K, Kim HG, et al. Ribosomal S6 kinase 2 is a key regulator in tumor promoter induced cell transformation. Cancer Res 2007;67:8104–12.
33. Lee-Fruman KK, Kuo CJ, Lippincott J, Terada N, Blenis J. Characterization of S6K2, a novel kinase homologous to S6K1. Oncogene 1999;18:5108–14.
34. Shima H, Pende M, Chen Y, Fumagalli S, Thomas G, Kozma SC. Disruption of the p70(s6k)/p85(s6k) gene reveals a small mouse phenotype and a new functional S6 kinase. EMBO J 1998;17:6649–59.
35. Phin S, Kupferwasser D, Lam J, Lee-Fruman KK. Mutational analysis of ribosomal S6 kinase 2 shows differential regulation of its kinase activity from that of ribosomal S6 kinase 1. Biochem J 2003;373: 583–91.
36. Li B, Chang CM, Yuan M, McKenna WG, Shu HK. Resistance to small molecule inhibitors of epidermal growth factor receptor in malignant gliomas. Cancer Res 2003;63:7443–50.
37. Fan QW, Knight ZA, Goldenberg DD, et al. A dual PI3 kinase/mTOR inhibitor reveals emergent efficacy in glioma. Cancer Cell 2006;9:341–9.